2013 IEEE/RSJ International Conference on
Intelligent Robots and Systems (IROS)
November 3-7, 2013. Tokyo, Japan

Telerobotic Palpation for Tumor Localization with Depth Estimation

A. Talasaz[1,3] and R.V. Patel[1,2,3]
[1]Department of Electrical & Computer Engineering, [2]Department of Surgery, The University of Western Ontario, and
[3]Canadian Surgical Technologies & Advanced Robotics (CSTAR)
London, Ontario, Canada.
atalasaz@uwo.ca , rvpatel@uwo.ca

Abstract— **This work is aimed at developing a new minimally invasive approach to characterize tissue properties in real time during telerobotic palpation and to localize tissue abnormality while estimating its depth. This method relies on using a minimally invasive probe with a rigidly mounted tactile sensor at the tip to capture the force distribution map and the indentation depth by each tactile element and thereby generating a stiffness map for the palpated tissue. The hybrid impedance control technique is used for this approach to enable the operator to switch between position control and force control and thereby to autonomously obtain the required information from the remote tissue. The operator would then be able to localize tissue abnormality based on the force distribution map, the tissue stiffness map and the indentation depth which are visually presented to him/her in real time. This method also enables the operator to estimate the depth at which the tissue abnormality is located. Our results show that tactile sensing alone may be unable to detect tumors embedded deep inside tissue and may also not be a good alternative for palpation on uneven tissue surfaces.**

I. Introduction

Tactile sensation is one of the main sources of haptic information that helps a surgeon to get feedback from tissue deformation and pressure distribution on the tissue during open surgery. Unlike in conventional open surgery, tissue is not directly accessible to the surgeon during Minimally Invasive Surgery (MIS). This prevents the clinician from localizing tumors by direct palpation in MIS [1], [2].

The main contribution of this work is a novel approach for integrating force control with tactile sensing and position control, to characterize tissue stiffness and to localize tumors while obtaining depth estimation for the tumors in MIS.

Several researchers have incorporated tactile sensors with laparoscopic instruments to enable surgeons to measure mechanical properties of tissue during MIS: Dargahi et al. [3] developed a tactile sensor for tumor localization for breast cancer. This non-invasive approach can predict the modulus of elasticity over breast tissue regardless of its thickness and thereby localize the embedded tumor. Wellman and Howe [4] used a tactile probe to estimate the size and the shape of a tumor in breast tissue. This work only relies on a pressure distribution map to detect tumor size and shape. Liu et al. [5] designed a force-sensitive wheeled probe using an ATI Nano17 force/torque sensor to explore the surface of tissue, collect force data in the palpation direction and combine them with the indentation depth information to characterize the stiffness of tissue. This method requires a preregistration of soft-tissue surfaces to estimate the indentation depth. Bicchi et al. [6] have developed a MIS sensorized laparoscopic instrument using strain gauges embedded inside the tool to measure the forces applied to the tip of the instrument and thereby to estimate the properties of the manipulated tissue. Although it can be used for lump detection, it cannot give any information about force distribution on tissue since it only measures a single-point force of the tool-tissue interaction. In [7], a miniaturized fiber optic sensor was designed to measure the interaction force and the indentation depth at the same time in a minimally invasive manner. However, it has a number of limitations in practice: Due to the small size of the probe tip, it would take a significant amount of time to palpate the entire tissue with the possibility of missing some areas. Besides, the probe can only detect tumors close to the surface of tissue (about $2mm$), therefore, it cannot be used for depth estimation.

The contribution of this paper is a novel approach for tumor localization in robotics-assisted minimally invasive surgery (RAMIS). This work characterizes tissue properties telerobotically while a tactile sensing instrument (TSI) [8] is inserted into the patient's body in a minimally invasive manner to collect position, tactile, and force data from the sensor-tissue interaction without encountering the problem of friction at the trocar. Using this approach, the operator would be able to localize tumors in 3D (tumor position in the tissue plane and its depth in the tissue) using the real time tissue stiffness map and the force distribution map generated based on the collected data from inside the body.

The outline of this paper is as follows. Section II introduces the master-slave setup used for this work and gives some details about the palpation probe used for tumor localization. The RAMIS control approach used in this work is explained in Section III. Experimental results are presented and discussed in Section IV.

II. Setup Description

Fig. 1 shows the master-slave teleoperation setup which consists of a Mitsubishi PA10-7C robot as the slave and a 7 Degrees-of-Freedom (DOFs) Haptic Wand [9] as the master interface (see [10], [11] for more details about the setup). At the robot end effector, a tactile sensing instrument (TSI),

This research was supported by the following grants awarded to Dr. R.V. Patel: the Ontario Centres of Excellence grant IC50272, the Natural Sciences and Engineering Research Council (NSERC) of Canada grants CRDPJ349675-06 and RGPIN1345; and the Canada Research Chairs Program.

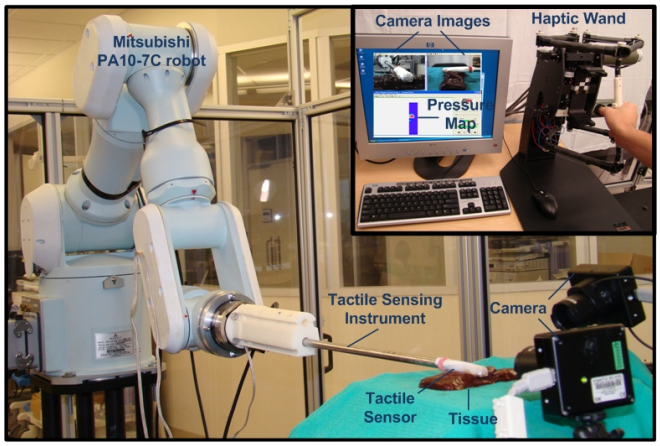

Fig. 1: Master-slave robotic setup palpating a tissue.

shown in Fig. 2, is used to measure the pressure distribution over tissue during tumor localization in soft-tissue palpation. The sensor used in this research is a two-dimensional array (15×4) of pressure sensing capacitive elements in a thin and continuous sheet developed for measuring the tactile pressure distribution between objects in direct physical contact. Each element is $2mm \times 2mm$ and the total size of the sensor is $30mm \times 8mm$ (see [12] for more information about the TSI). The main advantage of using this sensor is its capability of being inserted into the patient's body and being in direct contact with tissue to be palpated which makes it possible to capture the interaction between the tool and the tissue accurately without interfering with trocar-palpator friction. Visualization software has been developed in Simulink to display the pressure distribution in a color contour map. This software utilizes the visual color spectrum to indicate the levels of localized pressure intensity experienced by the probe, with dark red indicating the highest pressure intensity and blue indicating the lowest pressure intensity. A tumor may be distinguished from the surrounding tissue by the highest pressure area, because of its higher stiffness, indicated by the dark red color in the contour map. The sensitivity of the color contour map can also be adjusted in Simulink (once for all experiments). Moreover, this sensor is also used as the force sensor to measure the interaction force applied by the TSI on the tissue in the normal direction to the tissue plane (palpation direction).

III. The RAMIS Control Approach

A. Motivation

Fig. 3(a) and (b) show two examples where improper palpation on the tissue can cause large lateral forces on the tactile sensor. As a consequence, some elements of the TSI would be under higher pressure while some of them may not be in contact with the tissue. Higher pressure applied on those elements may be interpreted as a tumor and lead to false positives (see [12] for more information about the effect of lateral forces on tactile sensing tumor localization). Fig 3(c) also demonstrates a case with palpation on an uneven tissue surface. This is an example where the tactile sensor may lead to false positives/negatives even in a force

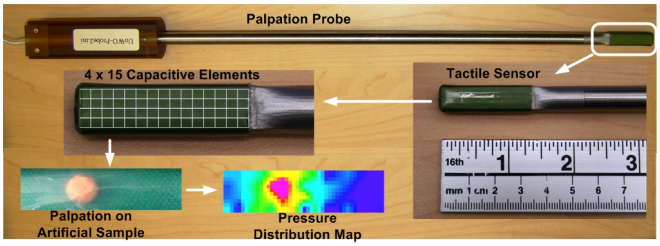

Fig. 2: Palpation probe (TSI).

controlled environment. In this example, there is a gap in the tissue being palpated which makes the tactile sensor not be in proper contact with the tissue. As a result, if a certain amount of force is applied on the tissue, the thick areas might be under higher pressure causing them to be interpreted as tumors. This example shows that when palpation is done on an uneven tissue surface, the tactile information collected from the tissue-sensor interaction may not be sufficient to localize tumor successfully. This problem occurs since the amount of deformation of the tissue has not been taken into account. On the other hand, success in tumor localization is highly dependent on how deep the tumor is located and if the tactile sensor is able to deform the tissue sufficiently to be sensitive to the underlying tumor. Using tactile information alone, the operator has no clue about the indentation depth to adjust the exploration force accordingly. The aforementioned problems provide the motivation for this work, i.e., (a) to develop a semiautonomous force control approach that applies different levels of exploration force consistently on tissue; (b) to capture tissue-sensor interaction data; and (c) to present them in real time during palpation in RAMIS to help the clinician to detect the position and the depth of a tumor in tissue.

B. Control Algorithm

Assuming that the diseased tissue is accessible for a clinician to palpate directly, the way the clinician detects a tumor is to put his/her finger on the tissue and to apply some force on the tissue to deform the tissue sufficiently to be sensitive to the underlying tumor. If the tumor is located near the surface of the tissue, he/she can detect it by his/her sense of touch (tactile feedback) while a small force is applied on the tissue, for a tumor in the middle of the tissue, more force is required to deform the tissue to let him/her feel the tumor and for a tumor at the bottom of the tissue, a significant amount of force is required for the clinician to detect the tumor. Therefore, in direct palpation, the clinician can get

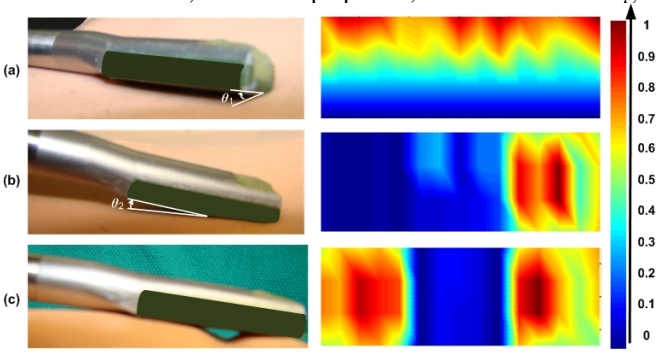

Fig. 3: Improper palpation cases using the TSI.

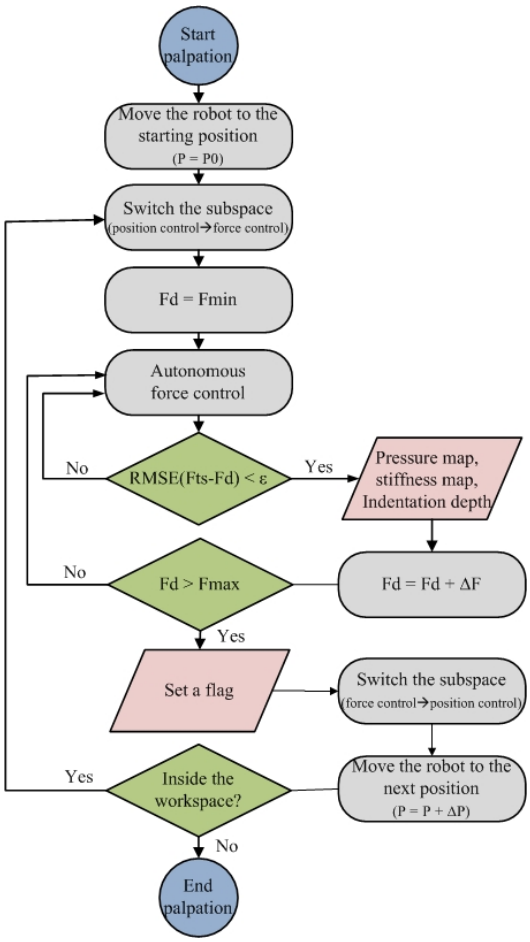

Fig. 4: Flowchart of the RAMIS control algorithm for tumor localization

some feeling about the depth of the tumor using his/her sense of touch (tactile feedback), the amount of force being applied to the tissue (force feedback), and the amount of deformation of the tissue (position data). In this work, we attempt to implement the same idea robotically and collect the force, tactile and position data using our robotic palpation setup.

If the force applied in the palpation direction is sufficient, then by using the color contour map of the pressure distribution obtained from the capacitive elements, we may be able to detect tumors in the tissue distinguished in dark red on the screen. By combining the position data with the force measurement for each element, we can also measure the stiffness of the tissue under that element and its indentation depth. By the linear elastic assumption of tissue, the stiffness of the tissue under each element can be evaluated by measuring the Young's modulus (modulus of elasticity) of that area as:

$$E_e = \frac{F_e L_{e0}}{A_{e0} dL_e} \tag{1}$$

where E_e is the Young's modulus of the tissue under the element, F_e is the force exerted by the element to the tissue, A_{e0} is the area of the element (4e-6), L_{e0} is the initial tissue thickness under that element, and dL_e is the amount of indentation depth measured through the kinematics of the robot. Using these information for all sixty elements of the sensor, we can then generate a stiffness map for the palpated area. The average of the indentation depths for all elements along with the total amount of force applied by the TSI can also be used to estimate the TSI indentation depth at that force level. At the same time, if an area is suspected to have a tumor, both the pressure map and the stiffness map can be used to localize that accurately, while estimating its depth using the indentation depth information. To achieve these objectives, we define two control subspaces at the slave side: one in the palpation direction which is defined as a direction perpendicular to the tissue surface and the other in the tissue plane (the surface of tissue). For the first subspace we need to control the position of the TSI until it reaches the top of the tissue. Then, we need a force control algorithm to apply a certain amount of force on the tissue and deform it appropriately to capture the required information for that area. To explore the tissue for possible tumors, we need position control of the TSI over the tissue plane. In order to palpate the tissue in a consistent manner, regardless of the thickness of the area being palpated or whether the surface of tissue is flat or uneven, we autonomously control the palpation force from a minimum value to a maximum, which are set based on the stiffness of the tissue being palpated, with δF increments to see at which level the embedded tumor is detected. For each level of force, when the root mean square of the error (RMSE) between the desired force (F_d) and the actual force measured by the tactile sensor (F_{ts}) is less than ϵ, then we record the force distribution measured by the tactile sensor and calculate the stiffness map and the indentation depth of the TSI. This procedure is repeated for all force levels. When the force applied by the TSI reaches F_{max}, a flag is set indicating that the palpation for that area is done and the operator can palpate another area. Fig. 4 summarizes the control algorithm in a flowchart.

C. Control Method

The control approach chosen for the slave manipulator is the Jacobian Inverse Hybrid Impedance Control (JI-HIC) [10]. The control problem here is to change the orientation of the TSI and its position along the palpation direction such that the palpation plane fully fits over the tissue plane, and then to palpate the tissue in x_t-y_t plane (position-controlled subspace). Moreover, the force applied on the palpation direction should be kept within a certain amount to ensure that palpation is consistent (force-controlled subspace). The JI-HIC method used for the slave manipulator attempts to generate a reference acceleration trajectory reflecting the desired forces along the force-controlled subspace and the desired impedance along the position-controlled subspace. This control method tries to regulate the force F_e while the robot is moving along a trajectory on the surface of the tissue looking for tumors. Equation (2) shows the reference acceleration trajectory for hybrid impedance control;

$$\begin{aligned}\ddot{\boldsymbol{X}}_r = \boldsymbol{M}_d{}^{-1}[&- \boldsymbol{F}_e + (\boldsymbol{I} - \boldsymbol{S})\boldsymbol{F}_d - \boldsymbol{B}_d(\dot{\boldsymbol{X}}_r - \boldsymbol{S}\dot{\boldsymbol{X}}_d) \\ &- \boldsymbol{K}_d\boldsymbol{S}(\boldsymbol{X}_r - \boldsymbol{X}_d))] + \boldsymbol{S}\ddot{\boldsymbol{X}}_d \end{aligned} \tag{2}$$

and

$$\boldsymbol{X}_r(0) = \boldsymbol{X}_s(0)\ ,\ \dot{\boldsymbol{X}}_r(0) = \dot{\boldsymbol{X}}_s(0), \tag{3}$$

where $\boldsymbol{X}_d$ is a 3×1 vector that represents the desired Cartesian position from the Haptic Wand, $\dot{\boldsymbol{X}}_d$, and $\ddot{\boldsymbol{X}}_d$ are the corresponding velocity and acceleration; $\boldsymbol{M}_d$ and $\boldsymbol{B}_d$ denote the desired mass and damping parameters; $\boldsymbol{F}_d$ and $\boldsymbol{F}_e$ are the desired force and environment contact forces; The matrix $\boldsymbol{S}$ denotes the selection matrix that defines the force- and position-controlled subspaces ($\boldsymbol{S} = \boldsymbol{I}$ for entirely position-controlled and $\boldsymbol{S} = \boldsymbol{0}$ for entirely force-controlled). In our application, we need S_z (selection factor corresponding to the palpation direction) to switch from 1 to 0 when the TSI reaches close to the surface of the tissue.

IV. Experiments

An experimental evaluation was performed to explore the performance of the proposed approach for tactile sensing tumor localization in RAMIS. In this section, we first present the tissue models used for the experiments. Then, we present our results and discuss them in detail.

A. Experimental Conditions

The tissue used for the experiments was made of silicone gel (Ecoflex0030 with Silicone thinner) with elastic modulus 20 KPa that was experimentally measured by conducting several palpations on the tumor-free areas and recording the force data and the amount of indentation. The spherical tumors used for the experiments were made of silicon gel (SORTA-Clear40) and were eight times harder than the tissue phantom. The diameter of the tumors was chosen to be $8mm$ - equal to the width of the TSI. For evaluating the performance of our approach in depth estimation, a rectangular shaped tissue phantom with a flat surface was chosen with three tumors embedded in the tissue at different depths: $2mm$, $7mm$, and $10mm$. Fig. 5 shows the dimensions of the tissue phantom, the exact locations of the tumors and the depths at which the tumors were embedded. To mimic a real palpation task in MIS, a tissue phantom with an uneven surface was also made in order to study how the proposed approach works in this scenario. We attempted to make a tissue phantom with a curved surface such that it covers all the problematic cases mentioned in Fig. 3. If we divide the tissue into three equal parts, left ($x = [0mm \ \ 24mm]$), middle ($x = [25mm \ \ 48mm]$), and right ($x = [49mm \ \ 72mm]$), the tissue has a half-cylinder bump in the first part ($y = [20mm \ \ 30mm]$) and a tumor at $x = 12mm$, $y = 15mm$, a flat surface for the second part with a tumor at $x = 36mm$, $y = 15mm$, and double half-cylinder bumps on the sides of the third part ($y = [0mm \ \ 10mm]$, $y = [20mm \ \ 30mm]$) with a tumor embedded at $x = 60mm$, $y = 15mm$ (right in the middle of the tissue gap). The average surface height along the Z-axis was $25mm$ with a variation of $5mm$. In this case, three tumors were embedded at the same depth (at a height of $20mm$ from the bottom of the tissue). For ease of use and to provide a wider range of motion during the experiments, the tissues were placed on a table and palpated in the left to right direction. The operator received some visual cues from the marked tissue on a monitor connected to a camera overlooking the tissue but it was not possible to discern the location of the lump in the tissue from the camera image. He was asked to palpate the tissue by the TSI through the master-slave teleoperation setup. He was then asked to palpate the tissue in a discontinuous mode in different steps; palpating the first area, raising the TSI off the tissue, moving to the next area and repeating this pattern. In order to avoid overlap between the adjacent palpated areas, the surface of the tissue phantom was also marked as shown in Fig. 5. A switch was provided to the operator enabling him to choose between position and force control subspaces for the palpation direction. For the other directions, the Mitsubishi PA10-7C was set to be in a position-controlled subspace commanded by the operator via the Haptic Wand. The operator was asked to turn the switch ON ($S_z = 1$) and bring the TSI on top of the starting position shown in Fig. 5 under position control then turn it OFF ($S_z = 0$) enabling the robot to approach the surface of the tissue under force control while maintaining the desired force level on the tissue in the palpation direction. During the experiments, the real-time stiffness map, and the force distribution map for the palpated area along with the indentation depth of the TSI were shown to the operator on a monitor. They were also recorded for use in generating the stiffness and the force distribution maps of the entire tissue at the end of palpation. When autonomous force control was completed for an area, a flag was set informing the operator that it is ready for palpation as the next area. The implementation of the controllers for the master-slave teleoperation setup was done on two Windows-based systems, one for the master and the other for the slave. Communication between the two computers was done using the User Datagram Protocol (UDP). All control algorithms were implemented on the QuaRC Real-Time software which automatically generates real-time code directly from Simulink designed controllers targeting Windows [9]. All of the controllers for the master and slave manipulators were implemented at a sampling frequency of 1 kHz. Communication between the master and the slave PCs and transmission of the force and position data were also made at the same rate.

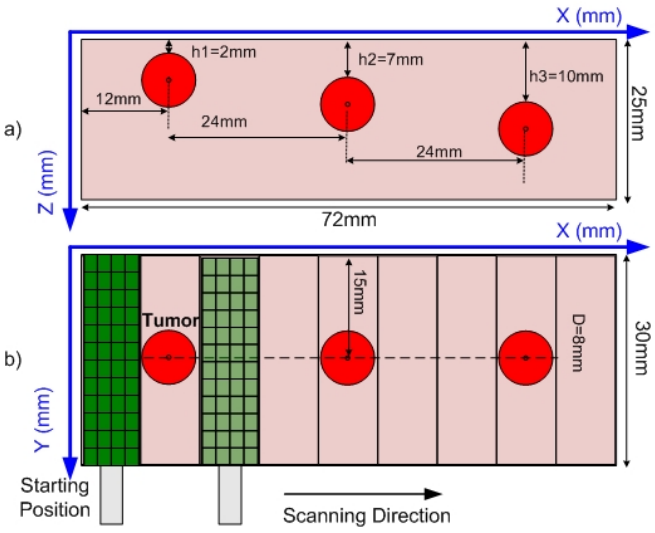

Fig. 5: Tissue model used for the experiments: a) side view; b) top view

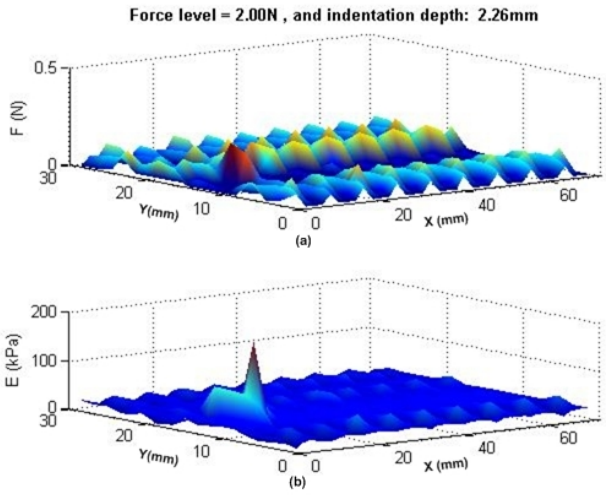

Fig. 6: The force distribution map (a) and the stiffness map (b) obtained via palpation with $2N$ exploration force.

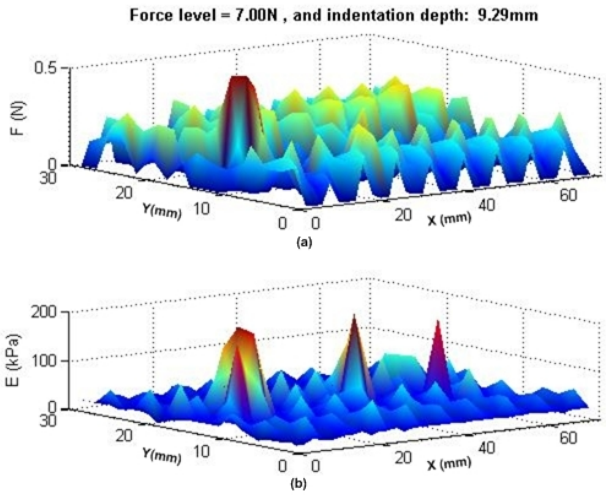

Fig. 8: The force distribution map (a) and the stiffness map (b) obtained via palpation with $7N$ exploration force.

B. Experimental Results

In the first experiment, we explored the effect of the proposed algorithm for tumor localization when the tumors were embedded at different depths. Figs. 6-9 show the experimental results for palpation on the tissue phantom shown in Fig. 5. In this experiment, we set the minimum and maximum exploration force to $1N$ and $7N$, respectively, with $1N$ increments. The results presented in Figs. 6-8 are those with the first observable change seen in the stiffness map. Fig. 6 shows the force distribution map and the stiffness map when the tissue was palpated with 2N exploration force. As can be seen, the only tumor that is detectable from the results with this amount of exploration force is the one embedded close to the tissue surface (at $2mm$). This tumor was detected with $2.26mm$ indentation depth of the probe. Fig. 7 shows the results for $5N$ exploration force at which the first change in stiffness was observed for the tumor embedded at $7mm$ depth (distinguished in yellow from the rest of the stiffness map). However, this tumor is not detectable from the force distribution map. The depth of the tumor was also estimated as $7.40mm$. Finally, with $7N$ exploration force, according to the results obtained from the stiffness map (Figs. 8, 9), all three tumors were found successfully. Our proposed algorithm detected the last peak in the stiffness map with $9.29mm$ indentation depth of the probe. However, as shown in Fig. 9, only one tumor that was embedded close to the tissue surface was detectable by using the force distribution map.

In our next experiment, we explored the performance of our approach for a tissue phantom with a curved surface. According to the results of the stiffness map obtained from palpation of this tissue phantom, all tumors were detected when $7N$ exploration force was applied in the palpation direction. Fig. 10 shows the force distribution map and the stiffness map for an average of $10.54mm$ indentation depth. Fig. 11 also shows the locations of the detected tumors in the force distribution map (top) and the stiffness map (bottom). All tumors were correctly detected from the stiffness map. However, it is hard to distinguish the tumors from the force distribution map shown in Fig. 11. Since the middle part of the tissue had a flat surface with a tumor

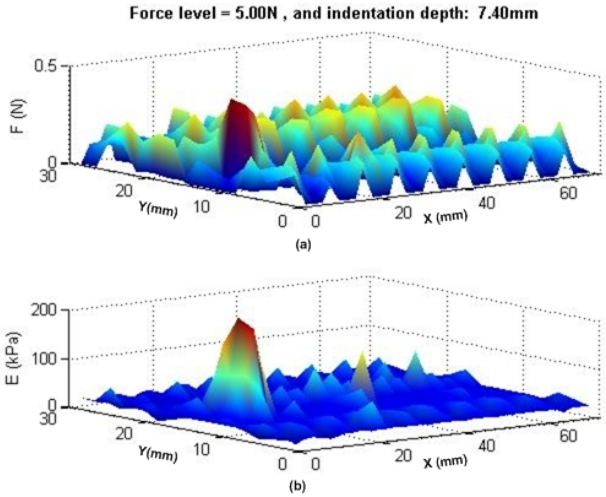

Fig. 7: The force distribution map (a) and the stiffness map (b) obtained via palpation with $5N$ exploration force.

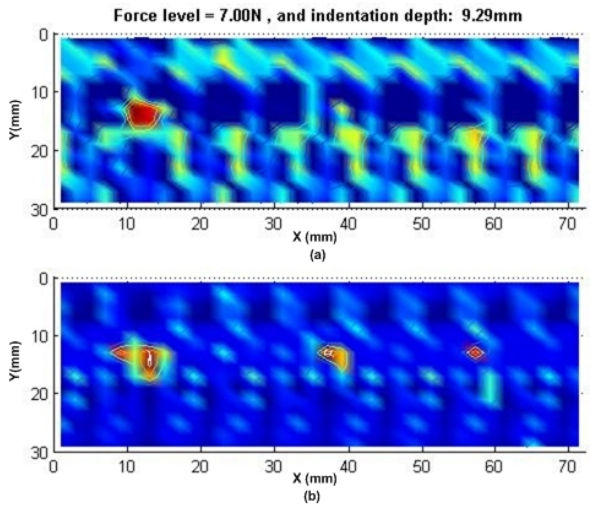

Fig. 9: Location of the tumors detected from the force distribution map (a) and the stiffness map (b) with $7N$ exploration force.

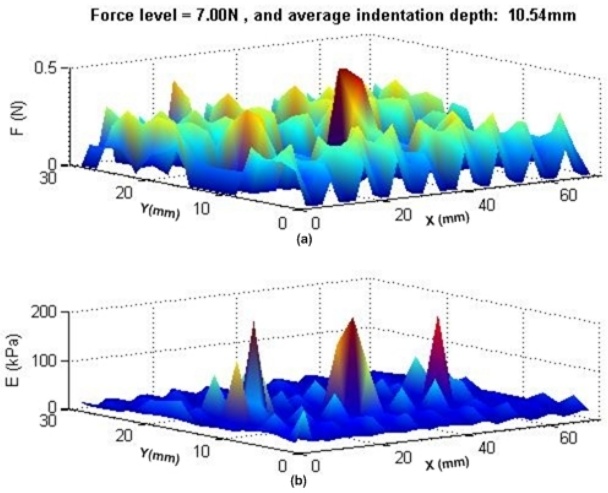

Fig. 10: The force distribution map (a) and the stiffness map (b) obtained via palpation on an uneven tissue surface with $7N$ exploration force.

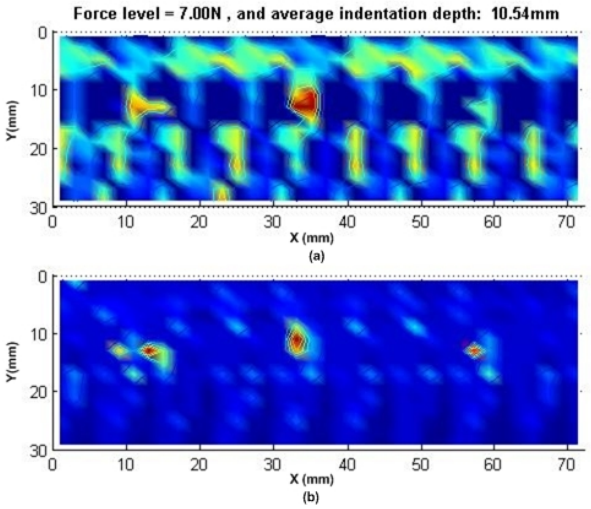

Fig. 11: Location of the tumors detected from the force distribution map (a) and the stiffness map (b) with $7N$ exploration force on an uneven tissue.

embedded at $x = 36mm,\ y = 15mm$ with $2mm$ depth, it was correctly distinguished in the force distribution map. However, the tissue bump in the first area of the tissue ($x = [0mm\ 24mm]$) prevented it from being easily located. Furthermore, the convex tissue surface of the third area caused the third tumor embedded at $x = 60mm,\ y = 15mm$ to be undetectable via the force distribution map.

C. Discussion

The results obtained for palpation of tissue on a flat surface with tumors embedded at different depths reveals that tactile sensing by itself is not capable of localizing tumors embedded deep inside tissue. However, if force distribution information is combined with the amount of tissue deformation, then the combined information can be successfully used to evaluate the stiffness of tissue and to detect stiffness changes in the resulting stiffness maps and thereby localizing tumors accurately. The deeper the TSI probe palpates the tissue phantom, the greater the stiffness changes in the stiffness map for the deep tumors embedded in the tissue. The results also show that the proposed algorithm was successful in estimating the tumor depth.

Furthermore, the results obtained from the second experiment clearly demonstrates the advantages of using the stiffness map for more accurate tumor localization over the force distribution map since both deformation and force distributions are taken into account in the stiffness map. However, since the force distribution map only contains information about the amount of force under the capacitive elements in the probe regardless of the thickness of the underlying tissue, it is possible to measure higher forces if the TSI probe palpates a thicker part of the tissue. In other words, the force distribution map provided by the probe cannot distinguish between palpation on the tumor and palpation on a thicker part of the tissue.

V. Acknowledgements

The Tactile Sensing Instrument used in the experimental work for this paper was designed at CSTAR in a project on palpation for minimally invasive surgery involving Melissa Perri, Greig McCreery, Ana Luisa Trejos, Michael Naish, Rajni Patel and Richard Malthaner. The authors would also like to thank Chris Ward for his help with tissue preparation.

References

[1] M. E. H. Eltaib and J. R. Hewit, "Tactile sensing technology for minimal access surgery a review," *Mechatronics*, vol. 13, pp. 1163–1177, 2003.

[2] M. V. Ottermo, M. Vstedal, T. Lang, Stavdahl, Y. Yavuz, T. Johansen, and R. Marvik, "The role of tactile feedback in laparoscopic surgery," *Surgical Laparoscopy Endoscopy and Percutaneous Techniques*, vol. 16, no. 6, pp. 390–400, 2006.

[3] J. Dargahi, S. Najarian, V. Mirjalili, and B. Liu, "Modeling and testing of a sensor capable of determining the stiffness of biological tissues," *Canadian Journal of Electrical and Computer Engineering*, vol. 32, no. 1, pp. 45–51, 2007.

[4] P. S. Wellman, , and R. D. Howe, "Extracting features from tactile maps," in *2nd International Conference on Medical Image Computing and Computer Assisted Intervention*, 1999, pp. 1133–1142.

[5] H. Liu, D. P. Noonan, B. J. Challacombe, P. Dasgupta, L. D. Seneviratne, and K. Althoefer, "Rolling mechanical imaging for tissue abnormality localization during minimally invasive surgery," *IEEE Transactions on Biomedical Engineering*, vol. 57, no. 2, pp. 404–414, Feb. 2010.

[6] A. Bicchi, G. Canepa, D. D. Rossi, P. Iacconi, and E. P. Scillingo, "A sensor-based minimally invasive surgery tool for detecting tissue elastic properties," in *IEEE International Conference on Robotics and Automation*, 1996, pp. 884–888.

[7] H. Liu, J. Li, X. Song, L. D. Seneviratne, and K. Althoefer, "Rolling indentation probe for tissue abnormality identification during minimally invasive surgery," *IEEE Transaction on Robotics*, vol. 27, no. 3, pp. 450–460, June 2011.

[8] M. T. Perri, A. L. Trejos, M. D. Naish, R. V. Patel, and R. Malthaner, "Initial evaluation of a tactile/kinesthetic force feedback system for minimally invasive tumor localization," *IEEE/ASME Transaction on Mechatronics*, vol. 15, no. 6, pp. 925–931, Dec 2010.

[9] Quanser. [Online]. Available: http://www.quanser.com

[10] A. Talasaz, "Haptics-enabled teleoperation for robotics-assisted minimally invasive surgery," Ph.D. dissertation, The University of Western Ontario, 2012.

[11] A. Talasaz and R. V. Patel, "Remote palpation to localize tumors using a robot-assisted minimally invasive approach," in *IEEE International Conference on Robotics and Automation*, 2012, pp. 3719–3724.

[12] A. Talasaz and R. Patel, "Integration of force reflection with tactile sensing for minimally invasive robotics-assisted tumor localization," *IEEE Transactions on Haptics*, vol. 6, no. 2, pp. 217–228, 2012.